ORIGINAL RESEARCH

QA1

QA2

CBX4 Regulates Long-Form Thymic Stromal Lymphopoietin–mediated Airway Inflammation through SUMOylation in House Dust Mite–induced Asthma

Shixiu Liang[1]*, Zicong Zhou[1]*, Changhui Yu[1]*, Zili Zhou[1], Jieyi Liu[1], Wufeng Huang[1], Hangming Dong[1], Fei Zou[2], Haijin Zhao[1], and Shaoxi Cai[1]

[1]Department of Respiratory and Critical Care Medicine, Chronic Airways Diseases Laboratory, Nanfang Hospital, and [2]Department of Occupational Health and Occupational Medicine, Guangdong Provincial Key Laboratory of Tropical Disease Research, School of Public Health, Southern Medical University, Guangzhou, Guangdong, China

Abstract

Thymic stromal lymphopoietin presents in two distinct isoforms: short-form (sfTSLP) and long-form (lfTSLP). lfTSLP promotes inflammation, whereas sfTSLP inhibits inflammation, in allergic asthma. However, little is known about the regulation of lfTSLP and sfTSLP during allergic attack in the asthma airway epithelium. Here, we report that SUMOylation was enhanced in house dust mite–induced allergic asthma airway epithelium. Inhibition of SUMOylation significantly alleviated airway T-helper cell type 2 inflammation and lfTSLP expression. Mechanistically, chromobox 4 (CBX4), a SUMOylation E3 ligase, enhanced lfTSLP mRNA translation, but not sfTSLP, through the RNA-binding protein muscle excess (MEX)-3B. MEX-3B promoted lfTSLP translation by binding the lfTSLP mRNA through its K homology domains. Furthermore, CBX4 regulated MEX-3B transcription in human bronchial epithelial cells through enhancing SUMOylation concentrations of the transcription factor TFII-I. In conclusion, we demonstrate an important mechanism whereby CBX4 promotes MEX-3B transcription through enhancing TFII-I SUMOylation and MEX-3B enhances the expression of lfTSLP through binding to the lfTSLP mRNA and promoting its translation. Our findings uncover a novel target of CBX4 for therapeutic agents for lfTSLP-mediated asthma.

Keywords: asthma; airway inflammation; TSLP; SUMOylation

1

Clinical Relevance

This study highlights the specific regulatory mechanisms of long-form thymic stromal lymphopoietin (lfTSLP). We identified that chromobox 4, a SUMOylation E3 ligase, is playing a critical role in lfTSLP, but not short-form TSLP, expression. Mechanistically, chromobox 4 regulates transcription of the RNA-binding protein MEX-3B by enhancing transcription factor SUMOylation levels of general transcription factor TFII-I, resulting in enhanced expression of lfTSLP through MEX-3B binding to the lfTSLP mRNA and promoting its translation.

(Received in original form July 14, 2021; accepted in final form December 6, 2021)

*These authors contributed equally to this work.

Supported by the National Natural Science Foundation of China (81700034, 81670026, 8147022, 81770033, and 81970032), Natural Science Foundation of Guangdong Province (2017A030310106, 2015A030313236, and 2017A030313849), and Precision Medicine Research of the National Key Research and Development Plan of China (2016YFC0905803).

Author Contributions: S.L. and Zicong Zhou wrote and edited the manuscript. Zili Zhou and J.L. performed the experiments and acquired data. W.H., H.D., and F.Z. analyzed the data. S.C., C.Y., and H.Z. designed the study and are accountable for all aspects of the work in ensuring that questions related to the accuracy or integrity of any part of the work are appropriately investigated and resolved. All authors reviewed and approved the final manuscript.

Correspondence and requests for reprints should be addressed to Shaoxi Cai, Ph.D., Department of Respiratory and Critical Care Medicine, Chronic Airways Diseases Laboratory, Nanfang Hospital, Southern Medical University, 1023-1063 Shatai Road, Baiyun District, Guangzhou, China. E-mail: hxkc@smu.edu.com.

This article has a data supplement, which is accessible from this issue's table of contents at www.atsjournals.org.

Am J Respir Cell Mol Biol Vol ■■, Iss ■■, pp 1–13, ■■ ■■ 2022

Originally Published in Press as DOI: 10.1165/rcmb.2021-0301OC on XXX
Internet address: www.atsjournals.org

~~CBX4~~Thymic stromal lymphopoietin (TSLP) is an IL-7–like factor and has been reported to be an important epithelium-derived factor involved in the initiation and remodeling of allergic airway inflammation (1). TSLP has been shown to contribute to T2-high inflammation by imparting its function on dendritic cells (2), innate lymphoid cells (3), eosinophils (4), and mast cells (5). In addition, TSLP has been demonstrated to function in neutrophilic T2-low airway inflammation by activating dendritic cells to induce a T-helper cell type 17 (Th17) phenotype (6). These data suggest that targeting TSLP might achieve broader effects. It has been reported that tezepelumab, an antibody targeting TSLP, significantly decreased symptoms in patients with uncontrolled moderate to severe asthma exacerbations, irrespective of baseline blood eosinophils (7). It has been demonstrated that TSLP exists in two distinct isoforms, long form (lfTSLP) and short form (sfTSLP), in human bronchial epithelial (HBE) cells (only full-length TSLP has been detected in mice) (8). Previous work by our laboratory and other laboratories found that sfTSLP functions in antimicrobial activity and in maintaining immune homeostasis, whereas lfTSLP promotes inflammation (9, 10). In epithelium challenged with polyinosinic-polycytidylic acid and house dust mite (HDM), lfTSLP expression was upregulated, whereas sfTSLP expression was unaffected (8, 11). Given that sfTSLP is composed of a 63–amino acid residue that is homologous to the C-terminal portion of lfTSLP, the role of sfTSLP should be kept in mind when proposing therapeutic drug strategies to block lfTSLP in patients with asthma. Therefore, it is critical to understand the specific regulatory mechanisms of lfTSLP.

~~SUMOylation~~ is an important post-translational modification implicated in many biological processes and diseases (12). Unlike polyubiquitylation, which facilitates protein degradation, SUMOylation regulates protein stability by affecting protein cellular localization and protein–protein or protein–DNA interactions (13). SUMOylation has been reported to regulate innate immunity and inflammatory responses by altering protein stability (14, 15), suggesting that SUMOylation might perform multiple functions in innate immunity and inflammatory responses via various substrates. The airway epithelium functions as an innate immunity barrier that can be activated by allergens through Toll-like receptor 3 and protease-activated receptor 2, thereby causing an increase in the expression of TSLP (16, 17). However, whether SUMOylation is involved in TSLP expression is unclear. Like ubiquitylation, SUMOylation is catalyzed by activating (E1), conjugating (E2), and ligating (E3) enzymes (18). Chromobox 4 (CBX4), a member of the polycomb repressive complexes (PRCs), is one of the ligases possessing nonpolycomb SUMOylation E3 ligase activities and polycomb function through its two SUMO-interacting motifs (SIM1/2) and chromodomain (CDM) in the N-terminus, respectively (19). CBX4 has been reported to function in a variety of cancers through SUMOylation or polycomb function (20, 21). However, the role of CBX4 in allergic inflammation has not been reported.

In the present study, we demonstrate that inhibition of SUMOylation alleviates airway inflammation and hyperreactivity in an experimental model of allergic asthma. Furthermore, we identified CBX4, a SUMOylation E3 ligase, as playing a critical role in the expression of lfTSLP but not sfTSLP. Mechanistically, CBX4 regulates transcription of the RNA-binding protein (RBP) muscle excess (MEX)-3B by enhancing transcription factor SUMOylation levels of general transcription factor II (TFII-I), resulting in enhanced expression of lfTSLP through MEX-3B binding to the lfTSLP mRNA and promoting its translation. Some of the results of these studies were previously reported in the form of a preprint (https://doi.org/10.1101/2021.05.24.445396).

Methods

Animal Experiments

All experimental animal protocols were approved by the animal care and use committee of Southern Medical University. Detailed protocols are provided in the Experimental Procedures section of the data supplement.

Assessment of Airway Hyperreactivity, Serum IgE, and Analysis of ~~BAL~~ Fluid

Details of the samples collected and data analysis are described in the Experimental Procedures section of the data supplement.

Histology

Lung tissue was fixed in 4% formaldehyde and embedded in paraffin, followed by cutting into sections for hematoxylin and eosin, periodic acid–Schiff, and immunohistochemical staining. Hematoxylin and eosin staining was used to assessed airway inflammation, and periodic acid–Schiff stain was used to assess mucus production. Expression of the target proteins was visualized by immunohistochemistry.

Cell Culture, Reagents, and Transfection

The HBE cell line HBE-135-E6E7 (~~Shaanxi~~ Fuheng Biotechnology) was used in this study. For HDM stimulation, 400 U/ml HDM (A4963; ALK-Abello A/S) was added to medium for 24 hours when cells reached a confluency of 70%. For 2-D08 or UNC3866 treatment, HBE cells were treated with 2-D08 (5, 10, or 20 μM) or UNC3866 (HY-100832, 50, 100, or 200 nM; MedChemExpress) for 24 hours, then 400 U/ml HDM was added for an additional 24 hours. After these treatments, HBE cells were harvested for subsequent experiments. For siRNA or plasmid transfection, Lipofectamine 3000 reagent (Thermo Fisher Scientific) was used to transfect siRNAs and plasmids according to the manufacturer's instructions. The siRNA sequence and plasmid information is listed in the Experimental Procedures section of the data supplement.

~~qRT-PCR~~, Western Blot, IP, and Immunofluorescence

Detailed protocols are described in the Experimental Procedures section of the data supplement.

Polyribosome Profile Analysis

Sucrose gradient fractionation was performed as previously described (22). Briefly, cells were treated with 100 μg/ml cycloheximide (HY-12320; MedChemExpress) at 15–30 minutes before harvesting. The cells were lysed with polysome lysis buffer, then centrifuged at 10,000 × *g* for 20 minutes at 4°C. The supernatant was added to the top of a 10–50% sucrose gradient. The gradients were centrifuged for 90 minutes in a SW41Ti swinging bucket rotor at 190,000 × *g* (~39,000 rpm) at 4°C and twelve 1-ml fractions were collected by upward replacement. The fractions were subjected to RNA isolation and ~~qRT-PCR~~ as mentioned above.

RNA IP Assay

An RNA IP assay was performed according to the instructions of the Magna RIP RNA-Binding Protein Immunoprecipitation Kit (MilliporeSigma). For detailed protocol information, *see* the Experimental Procedures section of the data supplement.

Chromatin IP Assay

A chromatin IP (ChIP) assay was performed according to the SimpleChIP Enzymatic Chromatin IP Kit instructions (9003; Cell Signaling Technology). For details, *see* the Experimental Procedures section of the data supplement.

Statistical Analysis

When comparing two groups, an unpaired two-tailed Student's *t* test (normal distribution data) was used to analyze the data. Multiple comparisons were carried out using one-way ANOVA followed by Bonferroni's test. Airway hyperreactivity (AHR) data were analyzed using two-way ANOVA. Data were analyzed with GraphPad Prism 6.0 software (GraphPad Software). The data were presented as mean ± SEM. Differences were considered statistically significant when the *P* value was less than 0.05.

Results

Inhibition of SUMOylation Attenuates Airway Th2 Inflammation

To determine whether an imbalance of SUMOylation/deSUMOylation occurs in asthma airway epithelium, we examined SUMO protein concentrations in an HDM-induced mouse model of asthma (Figure 1A). The results of immunohistochemistry show a significant increase in expression of SUMO1 and SUMO2/3 in HDM-induced allergic airway epithelium (Figure 1B). Similar results were observed in mouse lung protein extracts (Figure 1C). These observations indicated enhanced concentrations of SUMOylation in asthma airway epithelium. On the basis of these observations, we sought to address whether inhibition of SUMOylation may affect HDM-induced allergic airway inflammation. Mice were administered the SUMOylation inhibitor, 2-D08, before every challenge. In contrast to the mice treated with HDM only, HDM exposure induced much smaller peribronchial inflammatory cell infiltration and mucus production in the lungs of 2-D08–treated mice (Figures 1D and 1E). Consistent with these findings, leukocytes (eosinophils and neutrophils) (Figure 1F) and Th2 cytokines (IL-4 and IL-5) (Figure 1G) from BAL fluid and HDM-specific IgE (Figure 1H) in sera were reduced in 2-D08–treated mice. Furthermore, AHR was measured after exposure to increasing doses of methacholine. We observed that 2-D08–treated mice exhibited significantly reduced AHR compared with HDM-treated mice (Figure 1I). Collectively, these results show that SUMOylation was enhanced after exposure to HDM and that inhibition of SUMOylation can alleviate airway inflammation, mucus overproduction, and AHR.

lfTSLP Induction Was Suppressed in 2-D08–treated Asthma Mice and HBE Cells

In their study, Mitchell and colleagues reported that the airway epithelium is the main source of "alarmins" (e.g., IL-25, IL-33, and TSLP) in response to allergens (23). Thus, we sought to determine whether inhibition of SUMOylation may affect the expression of these cytokines. We observed that the protein concentrations of IL-25 and TSLP, but not of IL-33, were reduced in lung extracts of 2-D08–treated mice compared with those of HDM-treated mice (Figure 2A). To further investigate the effect of 2-D08 on the expression of "alarmins" in airway epithelium, we used lung histological sections stained for IL-25, IL-33, and TSLP. We found that only TSLP expression was attenuated in the airway epithelium of 2-D08–treated mice (Figures 2B–2D). These results indicate that inhibition of SUMOylation decreases TSLP expression in the airway epithelium.

In humans, TSLP exists in two distinct isoforms, lfTSLP and sfTSLP, whereas only full-length TSLP is found in mice (8). We therefore investigated the effect of SUMOylation on lfTSLP and sfTSLP expression in HBE cells. We observed a significant reduction of lfTSLP protein expression in 2-D08–treated HBE cells (Figure 2E). Because there is no commercial primary antibody specific to sfTSLP, we designed primers specific to sfTSLP to measure the level of mRNA expression. We found that 2-D08 had no effect on sfTSLP expression (Figure 2F). Unexpectedly, 2-D08 also did not affect lfTSLP mRNA expression (Figure 2F). This finding suggests that SUMOylation may regulate lfTSLP post-transcriptionally. Altogether, these observations suggest that SUMOylation functions in lfTSLP expression in asthma airway epithelium and HDM-treated HBE cells.

CBX4 Is Involved in the Regulation of lfTSLP Expression in HBE Cells

Given that E3 enzymes and ~~sentrin-specific~~ proteases show substrate specificity (18), they might be potential targets for therapeutic strategies (24, 25). Therefore, we performed qRT-PCR to evaluate the expression of SUMOylation E3 ligases and deSUMOylation enzymes. After exposure of HBE cells to HDM, we observed that the expression of SUMOylation E3 ligases was variably elevated, whereas deSUMOylation enzymes (~~sentrin-specific proteases~~) were unaffected (Figure 3A). Among the upregulated SUMOylation E3 ligases, we observed a significant increase in the expression of CBX4 and protein inhibitor of activated STAT1 (PIAS1) (Figures 3A and 3B). ~~Consistent with the IB data in HBE cells *in vitro*,~~ HDM-treated mice showed a higher expression of CBX4 in lung extracts and airway epithelium compared with PBS-treated cells (Figures 3C and 3D). To evaluate the effect of CBX4 and PIAS1, HBE cells were transfected with siRNAs targeting CBX4 and PIAS1, respectively. We observed that siRNA knockdown of CBX4 resulted in a significant decrease in the concentration of lfTSLP protein (Figure 3G). However, knockdown of PIAS1 did not affect the expression of lfTSLP (Figure 3H). Intriguingly, the degree of lfTSLP mRNA expression was unaffected in HBE cells after CBX4 or PIAS1 knockdown (Figures 3I and 3J). The discrepancy between the concentrations of lfTSLP protein and mRNA indicated that CBX4 might regulate the expression of lfTSLP post-transcriptionally. Collectively, these data suggest that the SUMOylation E3 ligase CBX4 functions in the regulation of lfTSLP protein expression in HDM-stimulated HBE cells.

CBX4 Is Involved in the Regulation of lfTSLP Translation

In addition to its function as a SUMOylation E3 ligase, CBX4 is also a member of the CBX protein family, which are canonical components of PRC1 that function as a transcription repressor (26). The N-terminal CDM and two SIMs (SIM1/2) of CBX4 contribute to PRC1 and SUMO E3 ligase-dependent functions, respectively

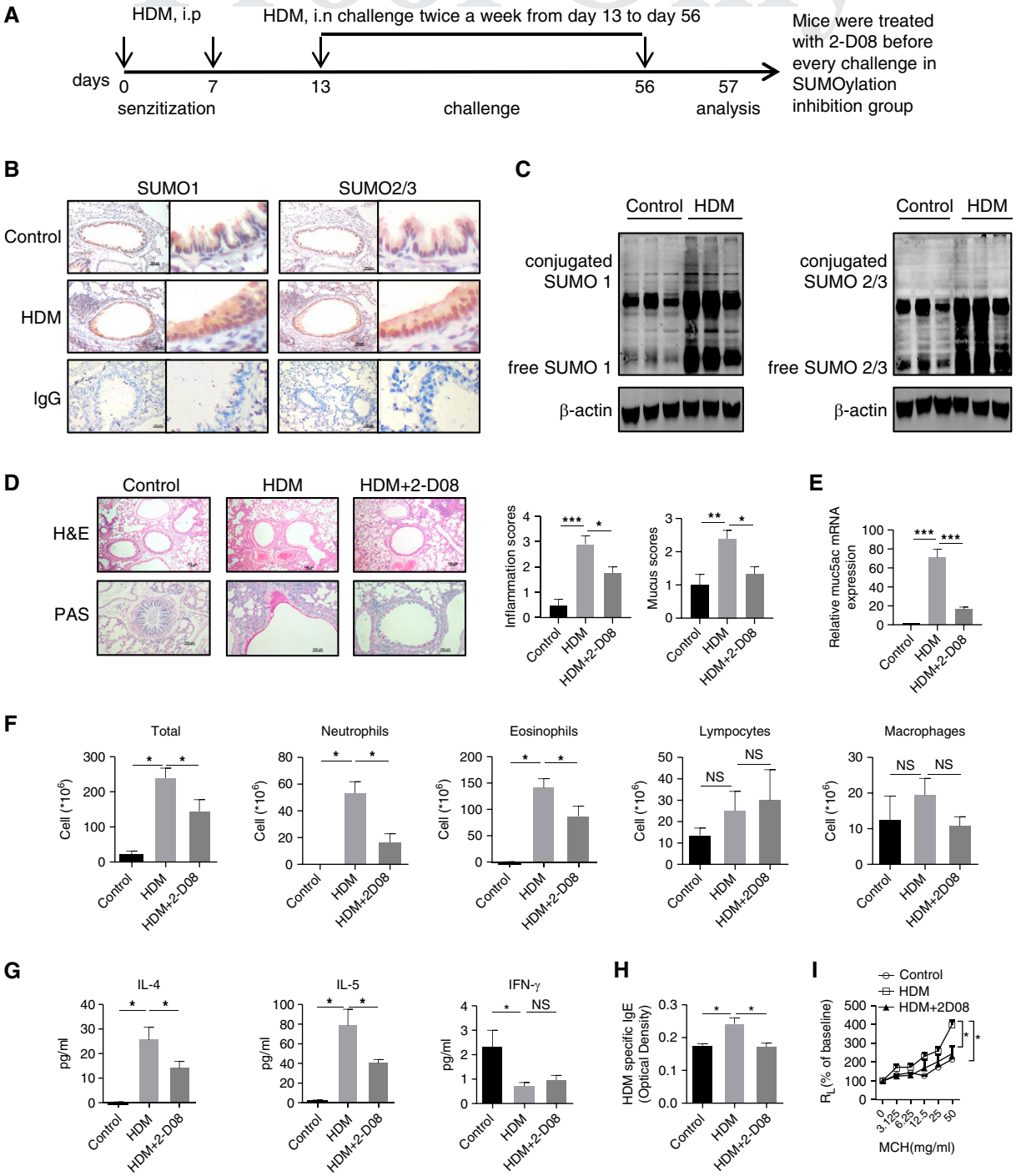

Figure 1. Inhibition of SUMOylation reduces house dust mite (HDM)-induced allergic asthma. (*A*) Mice were sensitized intraperitoneally (i.p) with 100 μl HDM or ~~PBS~~ on Days 0 and 7, then challenged intranasally (i.n) with 100 μl HDM or PBS from Day 13 to Day 56, and samples were collected on Day 57. Mice were treated with 2-D08 before every challenge in the SUMOylation inhibition group. (*B*) Lung sections were stained with ~~SUMO1~~ and ~~SUMO2/3~~ antibody by immunohistochemistry. (*C*) ~~IB~~ analysis of SUMO1 and SUMO2/3 in murine lung protein extract. (*D*) Lung sections were stained with hematoxylin and eosin (H&E) and periodic acid–Schiff (PAS) for assessing inflammation and mucus production. Quantification of inflammatory cell infiltration and airway mucus production in lungs was performed. (*E*) Muc5ac expression in mice lung extract was detected by ~~qRT-PCR~~. (*F*) Cells in BAL fluid were counted and classified after Wright-Giemsa staining. (*G*) Cytokines in BAL fluid were measured by ~~ELISA~~. (*H*) Serum HDM-specific IgE was measured using ELISA. (*I*) Invasive measurement of dynamic airway resistance in response to increasing doses of methacholine. Data are representative of two independent experiments with at least five mice per group and are presented as mean ± SEM. (*D–H*) One-way ANOVA with Bonferroni's *post hoc* test was used. (*I*) Two-way ANOVA was used. $^{*}P < 0.05$, $^{**}P < 0.01$, and $^{***}P < 0.001$. Scale bars, 100 μm. NS = not significant.

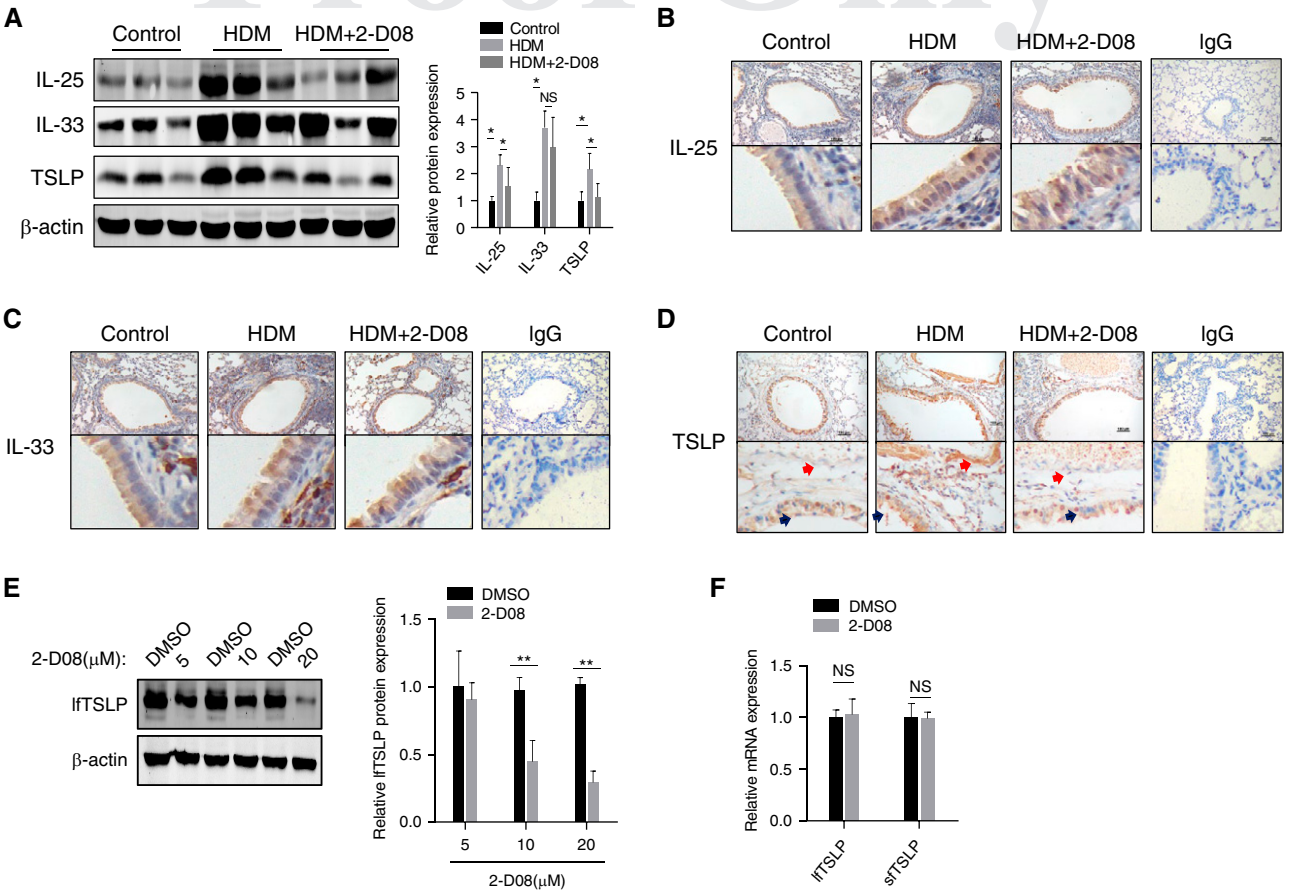

Figure 2. Inhibition of SUMOylation reduces long-form thymic stromal lymphopoietin (lfTSLP) protein expression. (*A*) IB analysis of IL-25, IL-33, and TSLP in murine lung protein extract. (*B–D*) Lung sections were stained with IL-25 (*B*), IL-33 (*C*), and TSLP antibody by immunohistochemistry (~~*D*~~). Epithelial cells (black arrows) and endothelial cells (red arrows) are indicated. (*E*) lfTSLP protein concentrations were detected by Western blotting in human bronchial epithelial (HBE) cells treated with different concentrations of 2-D08. (*F*) lfTSLP and short-form TSLP (sfTSLP) mRNA expression in HBE cells treated with 20 μM 2-D08 was measured by ~~RT-PCR~~. Data are presented as mean ± SEM. Images show representative results for one of three or more experimental replicates. (*A*) One-way ANOVA with Bonferroni's *post hoc* test was used. (*E* and *F*) Unpaired two-tailed Student's *t* test was used. $^{*}P < 0.05$ and $^{**}P < 0.01$. Scale bars, 100 μm.

17

(Figure 4A). To investigate whether the effect of CBX4 in lfTSLP expression depends on its function in PRC1 or as a SUMO E3 ligase, we measured the expression of lfTSLP in HBE cells after transfection with CBX4 plasmids bearing mutants in its CDM or SIM (ΔSIM1/2) (Figure 4A). We observed that ectopic expression of wild-type (WT) CBX4 and CDM-CBX4 significantly increased the concentration of lfTSLP protein, whereas ΔSIM1/2-CBX4 failed to do so (Figure 4B). This result suggests that CBX4 regulates lfTSLP through its SUMOylation function. This is consistent with the reduced concentration of lfTSLP protein observed in 2-D08–treated HBE cells (Figure 2C). In contrast, HBE cells treated with UNC3866, an inhibitor of the CBX4 CDM–histone interaction domain, did not affect lfTSLP expression compared with control (Figure 4C). Furthermore, these plasmid transfections did not affect lfTSLP mRNA expression in HBE cells (Figure 4D). These data indicate that SIM1/2, but not the CDM of CBX4, is required for ~~its~~ regulation of lfTSLP expression.

As mentioned above, the effect of CBX4 on lfTSLP expression was SIM1/2 dependent. To explore whether lfTSLP was regulated through CBX4-mediated SUMOylation directly, we performed IP to determine whether there is an interaction between CBX4 and lfTSLP. Unexpectedly, no interaction between these two proteins was observed (Figure 4E). Furthermore, HBE cells treated with the protein synthesis inhibitor cycloheximide presented a rate of degradation of lfTSLP protein similar to that of siCBX4 or the negative siRNA transfection group (Figure 4F). These results indicate that CBX4 does not regulate lfTSLP expression post-translationally. We therefore speculated that CBX4 might affect mRNA translation of lfTSLP. As mentioned above, CBX4 knockdown in HBE cells resulted in reduced concentrations of lfTSLP protein, whereas lfTSLP mRNA concentrations were unaffected. Furthermore, we treated HBE cells with the RNA polymerase II inhibitor actinomycin D for different time intervals with or without CBX4 knockdown. We observed that knockdown of CBX4 did not affect lfTSLP mRNA degradation in HBE cells compared with the control group (Figure 4G). In addition, to determine whether CBX4 affects lfTSLP translation, we performed polysome fractionation to analyze lfTSLP mRNA distribution profiles through sucrose gradients to separate ribosomal subunits (40S and 60S), monosomes (80S),

8

9

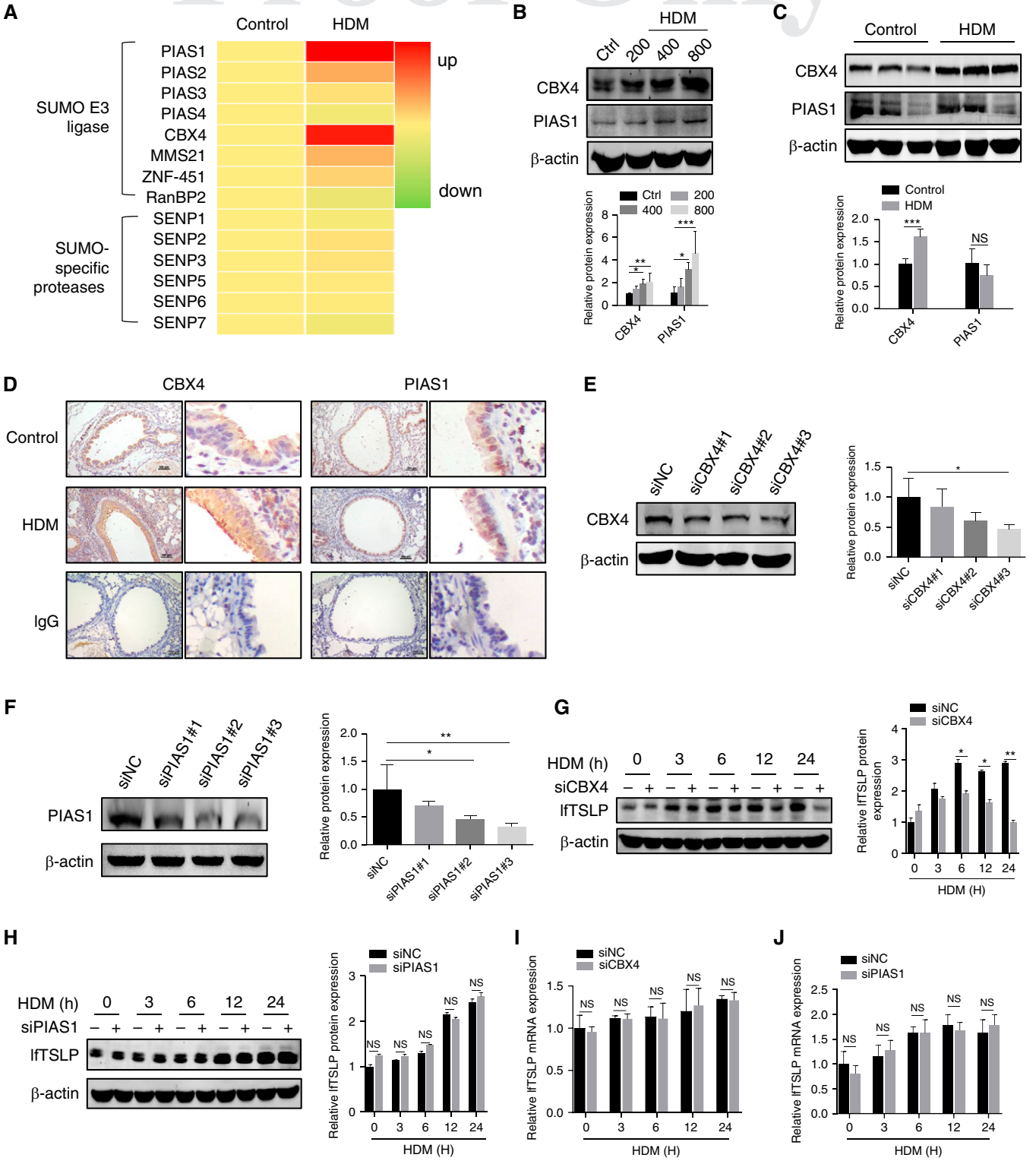

Figure 3. SUMOylation E3 ligase chromobox 4 (CBX4) regulates lfTSLP protein expression. (*A*) HBE cells were stimulated with 400 U of HDM for 24 hours, and the expression of SUMOylation E3 ligases (protein inhibitor of activated STAT1–4 [PIAS1–4], CBX4, MMS21, ZNF451, and RanBP2) and deSUMOylation enzyme sentrin-specific proteases were measured by ~~qRT-PCR~~. (*B* and *C*) CBX4 and PIAS1 protein concentrations were measured by Western blotting in HDM-treated HBE cells (*B*) and murine lung protein extracts (*C*). (*D*) Lung sections were stained with CBX4 and PIAS1 antibody by immunohistochemistry. (*E* and *F*) siCBX4 and siPIAS1 interference efficiency was detected by Western blot analysis. (*G–J*) lfTSLP protein and mRNA expression were detected at 3, 6, 12, and 24 hours of stimulation with HDM after CBX4

18

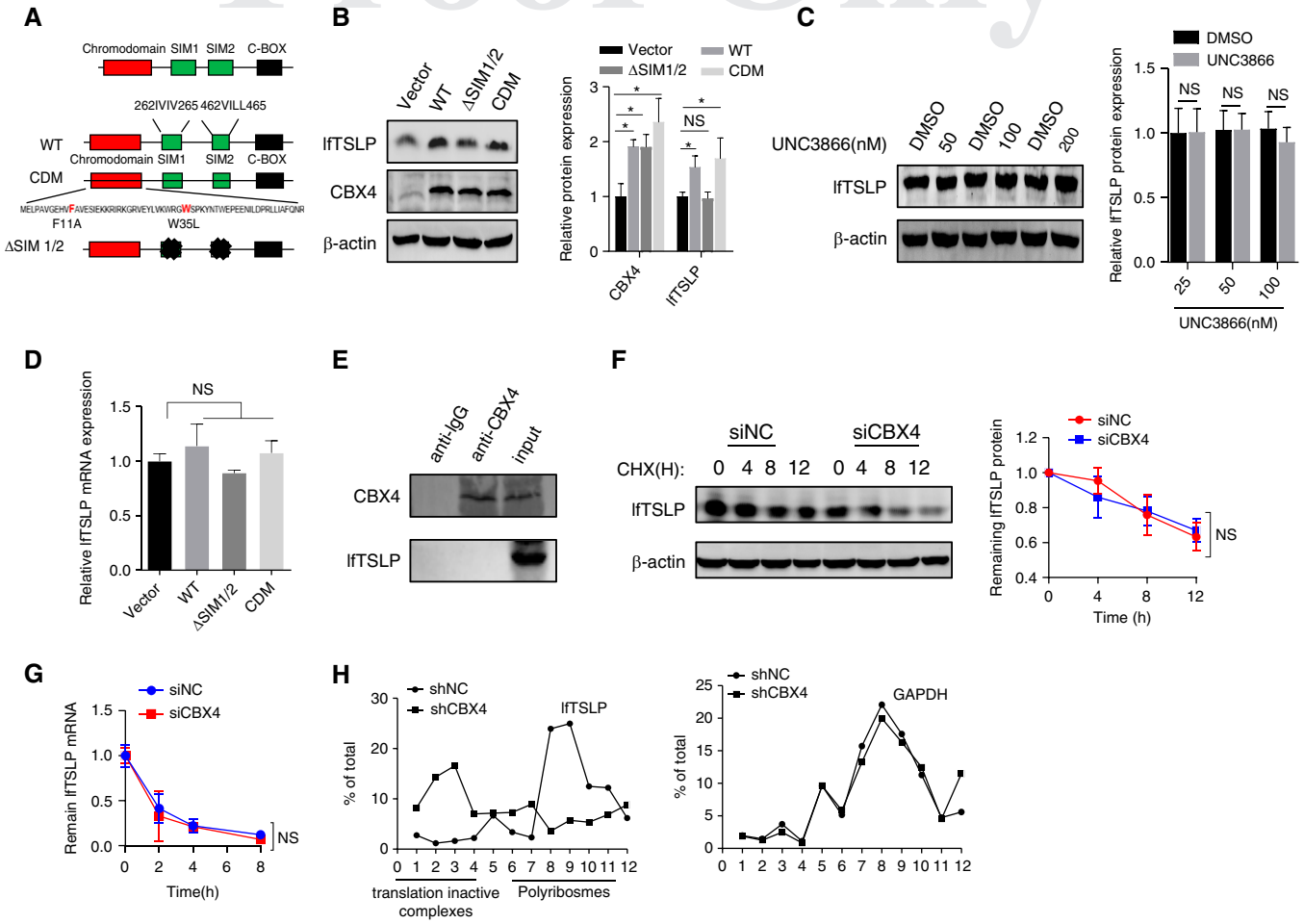

Figure 4. CBX4 regulates lfTSLP protein translation. (*A*) Schematic sketches of wild-type (WT) CBX4 and its mutants. (*B*) IB for the indicated proteins in HBE cells ectopically expressing the WT or CBX4 mutants for 48 hours. (*C*) HBE cells were treated with the indicated concentrations of UNC3866 for 24 hours. Expression of lfTSLP was determined by IB analysis. (*D*) HBE cells were transfected with WT or CBX4 mutant plasmids for 48 hours, and lfTSLP mRNA expression was determined by ~~qRT-PCR~~. (*E*) HDM-treated HBE lysates were subjected to IP with anti-CBX4 antibody or anti-IgG antibody followed by IB analysis with anti-lfTSLP antibody. (*F*) ~~siNC~~ or siCBX4 was transfected into HBE cells, followed by treatment with 100 μg/ml cycloheximide (CHX) for the indicated amount of time. Expression of lfTSLP was determined by IB analysis. (*G*) siNC or siCBX4 was transfected into HBE cells, followed by treatment with 5 μg/ml actinomycin D for the indicated amount of time. The lfTSLP mRNA expression was measured by ~~RT-PCR~~. (*H*) HBE cells transfected with shNC or shCBX4 were fractionated into cytoplasmic extracts through sucrose gradients. The distribution of lfTSLP and GAPDH mRNAs was quantified by ~~RT-PCR~~ analysis of RNA isolated from 12 gradient fractions. Data are presented as mean ± SEM. Images show representative results for one of three or more experimental replicates. (*B*) One-way ANOVA with Bonferroni's *post hoc* test was used. (*C* and *D*) Unpaired two-tailed Student's *t* test was used. (*F* and *G*) Two-way ANOVA was used. $^{*}P < 0.05$.

19

and progressively larger polysomes in HBE cells subjected to CBX4 siRNA transfection. Each group was divided into 12 fractions, and the concentrations of lfTSLP and GAPDH mRNA were assessed by qRT-PCR analysis. After CBX4 knockdown in HBE cells, we observed that lfTSLP mRNA shifted from fractions enriched for translating polyribosomes (fractions 5–12), indicative of enhanced translation, to fractions containing translation-dormant complexes, including messenger ribonucleic proteins, ribosome subunits, and monosomes (fractions 1–4) (Figure 4H). Overall, these results support the idea that CBX4 enhances lfTSLP translation without affecting its mRNA stability in HDM-treated HBE cells.

CBX4 Promotes lfTSLP Translation through the RBP MEX-3B

It has been reported that RBPs are essential for post-transcriptional gene regulation, linking RNA transcription, splicing, export, rate of translation, and stability (27, 28). In all of these processes, RBPs coordinate the regulation of the amount of protein produced from mRNA transcript. To

10

Figure 3. (*Continued*). or PIAS1 silencing. Data are presented as mean ± SEM. Images show representative results for one of three or more experimental replicates. (*B* and *E–J*) One-way ANOVA with Bonferroni's *post hoc* test was used. (*A* and *C*) Unpaired two-tailed Student's *t* test was used. $^{*}P < 0.05$, $^{**}P < 0.01$, and $^{***}P < 0.001$. Scale bars, 100 μm.

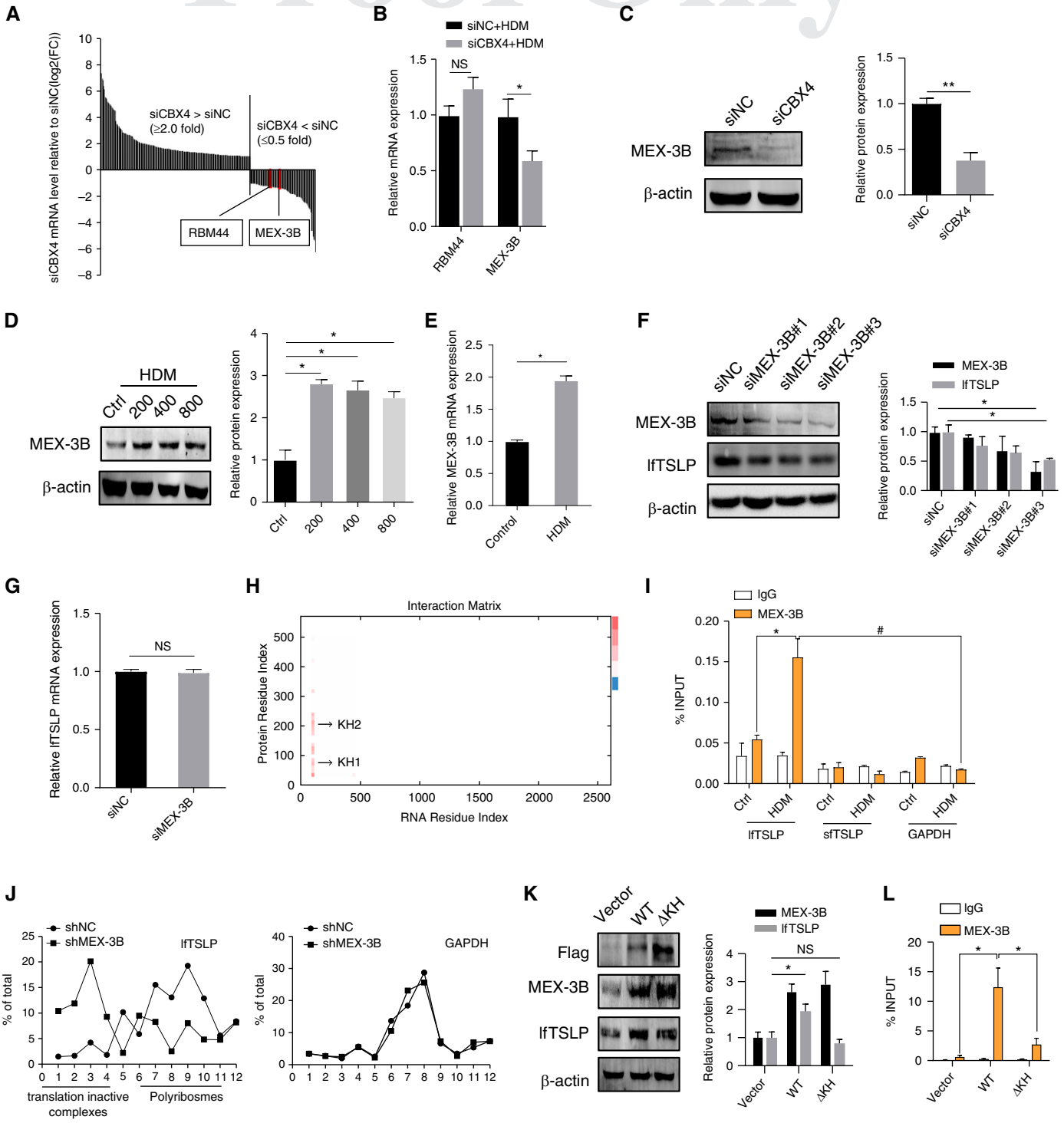

Figure 5. CBX4 regulates lfTSLP protein translation through muscle excess (MEX)-3B. (*A*) HBE cells were transfected with siNC or siCBX4 and subjected to mRNA sequencing. There were 197 upregulated and 86 downregulated genes. Among the 86 downregulated genes, there were two RNA-binding proteins: MEX-3B and RBM44. (*B*) Expression of MEX-3B and RBM44 was validated by qRT-PCR in HBE cells transfected with siNC or siCBX4. (*C*) HBE cells were transfected with siNC or siCBX4. MEX-3B protein expression was determined by IB analysis. (*D* and *E*) HBE cells were stimulated with HDM and MEX-3B protein, and mRNA concentrations were measured by IB analysis and qRT-PCR, respectively. (*F* and *G*) siNC or siMEX-3B was transfected into HBE cells. Expression of lfTSLP protein and mRNA was measured by IB analysis and qRT-PCR, respectively. (*H*) The potential binding sites of MEX-3B protein and lfTSLP mRNA were predicted by the catRAPID database. (*I*) qRT-PCR analysis of lfTSLP and sfTSLP mRNA that coimmunoprecipitated with mouse IgG or anti–MEX-3B antibody in HBE cells. GAPDH mRNA was used as a negative control. (*J*) HBE cells transfected with shNC or shMEX-3B were fractionated into cell extracts through sucrose gradients.

determine whether CBX4 regulates lfTSLP translation through RBPs, HBE cells transfected with CBX4 siRNA and control siRNA were subjected to whole-transcriptome sequencing. Sequencing analysis revealed that a total of 283 genes (197 upregulated and 86 downregulated) were significantly changed in HBE cells transfected with CBX4 siRNA targeting compared with control. Included in the 86 downregulated genes were MEX-3B and RBM44 (Figure 5A), two RBPs that play an important role in post-transcriptional gene regulation and are implicated in a number of diseases (29, 30). Interestingly, qRT-PCR analysis confirmed that MEX-3B, but not RBM44, was regulated by CBX4 (Figure 5B). In addition, MEX-3B protein expression decreased after CBX4 knockdown in HBE cells (Figure 5C). Furthermore, we observed that MEX-3B was upregulated in HDM-stimulated HBE cells (Figures 5D and 5E).

MEX-3B is a member of the MEX-3 family, which comprises MEX-3A, MEX-3B, MEX-3C, and MEX-3D. It has been reported that the MEX-3 family of proteins bind to specific mRNAs using two K homology (KH)-type RNA recognition domains and regulate the expression of their target proteins (31). Therefore, we also explored whether the other MEX-3 family proteins were regulated by CBX4, and we found that CBX4 knockdown had no effect on the expression of MEX-3A, MEX-3C, and MEX-3D (*see* Figure E1 in the data supplement). However, whether MEX-3B is involved in the post-transcriptional regulation of lfTSLP remains unclear. To determine if MEX-3B is involved in the post-transcriptional regulation of lfTSLP, lfTSLP protein and mRNA levels were measured in HBE cells transfected with siRNAs targeting MEX-3B. We observed that lfTSLP protein expression, but not mRNA expression, was significantly decreased after MEX-3B knockdown (Figures 5F and 5G). To address whether MEX-3B exerts its effect through binding to lfTSLP mRNA, we predicted the potential binding sites between the MEX-3B protein and lfTSLP mRNA using the catRAPID protein–RNA interaction database. The results of the analysis indicated that MEX-3B may interact with the 5′ untranslated region (UTR) of lfTSLP mRNA through its KH domains (Figure 5H). To confirm this prediction, lysates from HDM-treated HBE cells were subjected to IP with an MEX-3B primary antibody, then the degree of association of lfTSLP mRNA with the complexity was assessed by qRT-PCR. We observed that the MEX-3B protein interacted with the lfTSLP mRNA, but not the sfTSLP mRNA, and that the interaction was enhanced upon HDM stimulation (Figure 5I). Furthermore, knockdown of MEX-3B repressed lfTSLP translation (Figure 5J). To determine whether MEX-3B facilitates lfTSLP mRNA translation in a KH domain–dependent manner, HBE cells were transfected with plasmids encoding WT MEX-3B or a KH domain mutant MEX-3B (△KH). We observed a significant increase in lfTSLP protein concentrations in HBE cells transfected with WT MEX-3B, whereas no change was observed in the KH domain mutant (Figure 5K). In addition, the MEX-3B KH domain mutant exhibited a lower degree of association with the lfTSLP mRNA compared with WT MEX-3B (Figure 5L). These data suggest that CBX4 promotes lfTSLP translation through the RBP MEX-3B and that MEX-3B binds to the lfTSLP mRNA through its KH domains.

Transcription Factor TFII-I Binds the MEX-3B Promoter

As mentioned above, CBX4 regulates MEX-3B mRNA and protein expression. In addition, CBX4 knockdown in HBE cells treated with actinomycin D did not affect lfTSLP mRNA degradation compared with the control group (Figure 6A). This suggested that CBX4 may regulate the transcription of MEX-3B, and we speculated that CBX4 may directly bind to the MEX-3B promoter. Thus, we scanned the potential binding sites between CBX4 and the MEX-3B promoter through the hTFtarget database. Unfortunately, no potential binding sites were identified on the MEX-3B promoter (Figure E2). Furthermore, we found that the CBX4–histone interaction inhibitor, UNC3866, failed to alter MEX-3B expression (Figure 6B). These data suggest that CBX4 likely does not function as a transcription factor of MEX-3B by binding directly to its promoter.

Therefore, we hypothesized that CBX4 might function as a transcriptional coactivator of MEX-3B. To confirm this, we first used the ALGGEN database to predict the transcription factors that might bind to the promoter of MEX-3B. The results identified 17 potential transcription factors of MEX-3B (Figure E3). Next, we conducted an interaction prediction between CBX4 and these factors through GENEMANIA. Intriguingly, only TFII-I, encoded by *GTF2I*, was predicted to interact with CBX4 (Figure 6C), and this interaction was confirmed by IP (Figures 6D and 6E). Similarly, colocalization of CBX4 and TFII-I was also observed upon HDM stimulation in HBE cells (Figure 6F). Next, we investigated whether TFII-I could regulate MEX-3B expression. Knockdown of TFII-I resulted in a significant decrease of MEX-3B protein and mRNA concentrations (Figures 6G and 6H). To validate TFII-I as a transcription factor of MEX-3B, HBE cells treated with HDM were subjected to ChIP. Because the database indicated five major potential TFII-I binding sites in the MEX-3B promoter region, five MEX-3B promoter-specific primers covering these sites were designed for qRT-PCR. The results of the ChIP assay identified binding of TFII-I to the MEX-3B promoter (−680 to −751), which was significantly enhanced after HDM stimulation (Figure 6J). Furthermore, we observed that overexpression of TFII-I promoted transcriptional activity of MEX-3B using a luciferase reporter assay (Figure 6K). These results suggest that TFII-I is a transcriptional activator of MEX-3B.

CBX4-mediated TFII-I SUMOylation Enhanced the Transcription of MEX-3B

Previous studies have demonstrated that the transcriptional activity of TFII-I could be enhanced by SUMOylation (32). Therefore,

Figure 5. (*Continued*). The distribution of lfTSLP and GAPDH mRNAs was quantified by qRT-PCR analysis of RNA isolated from 12 gradient fractions. (*K*) IB for the indicated proteins in HBE cells transfected with control vector, Flag-tagged MEX-3B, or Flag-tagged MEX-3B-mutKH. (*L*) qRT-PCR analysis of lfTSLP mRNA coimmunoprecipitated with mouse IgG or anti-MEX-3B antibody in HBE cells transfected with control vector, Flag-tagged MEX-3B, or Flag-tagged MEX-3B-mutKH. Data are presented as mean ± SEM. Images show representative results for one of three or more experimental replicates. (*B*, *C*, *E*, and *G*) Unpaired two-tailed Student's *t* test was used. (*D*, *F*, *I*, *K*, and *L*) One-way ANOVA with Bonferroni's *post hoc* test was used. $^{*}P < 0.05$ and $^{**}P < 0.01$.

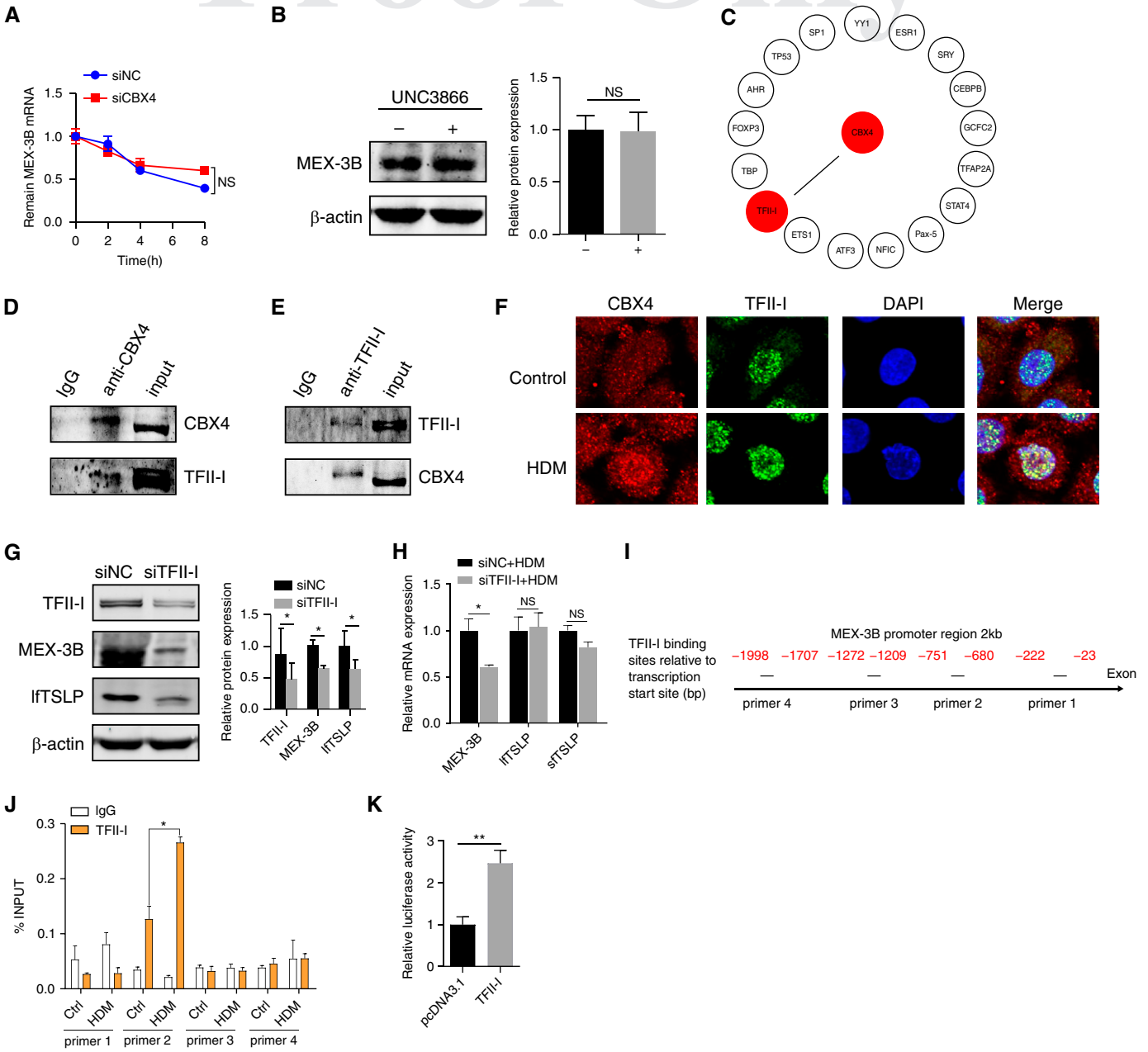

Figure 6. TFII-I is a transcriptional activator of MEX-3B. (*A*) siNC or siCBX4 was transfected into HBE cells, followed by treatment with 5 μg/ml actinomycin D for the indicated amount of time. MEX-3B mRNA expression was measured by ~~qRT-PCR~~. (*B*) HBE cells were treated with UNC3866 (200 nM) for 24 hours. The MEX-3B protein concentration was determined by IB analysis. (*C*) Potential transcription factors were scanned by the ALGGEN database. Prediction of an interaction between CBX4 and these factors was conducted by GeneMANIA. (*D*) HBE cell lysates were subjected to IP with anti-CBX4 antibody or anti-IgG antibody followed by IB analysis with anti-CBX4 and TFII-I antibody. (*E*) HBE cell lysates were subjected to IP with anti–TFII-I antibody or anti-IgG antibody followed by IB analysis with anti–TFII-I and CBX4 antibody. (*F*) Colocalization of CBX4 and TFII-I was analyzed by immunostaining of HBE cells with anti-CBX4 and TFII-I via confocal microscopy. (*G*) IB for the indicated proteins in HBE cells transfected with siNC or siTFII-I. (*H*) ~~qRT-PCR~~ for the indicated mRNA expression levels in HBE cells transfected with siNC or siCBX4. (*I*) Localization of TFII-I binding sites in MEX-3B promoter. (*J*) HBE cells were treated with 400 U of HDM 24 hours followed by chromatin IP with anti–TFII-I antibody or nonrelated IgG. Precipitated DNAs were quantified by ~~qRT-PCR~~ using five MEX-3B promoter-specific primers covering five TFII-I binding sites. (*K*) Human 293T cells transfected with pcDNA3.1(+)-TFII-I together with firefly luciferase reporter and pRL-tk-Renilla plasmids for 24 hours. Data are presented as mean ± SEM. Images show representative results for one of three or more experimental replicates. (*A*) Two-way ANOVA was used. (*B*, *G*, *H*, and *K*) Unpaired two-tailed Student's *t* test was used. (*J*) One-way ANOVA with Bonferroni's *post hoc* test was used. $^{*}P < 0.05$ and $^{**}P < 0.01$.

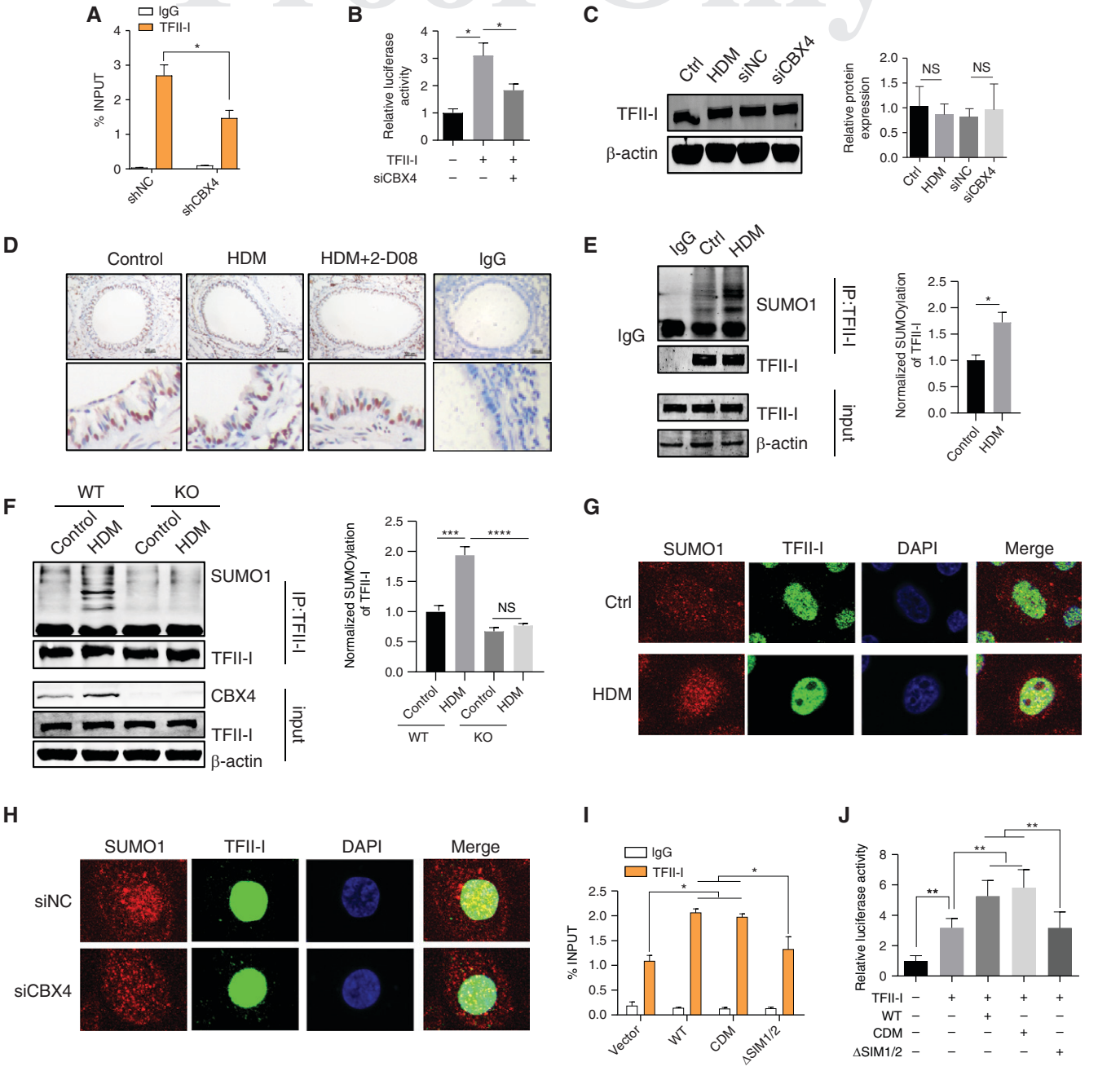

Figure 7. CBX4 regulates TFII-I transcriptional activity through SUMOylation. (*A*) HBE were transfected with shNC or shCBX4 followed by ChIP with anti–TFII-I antibody or IgG. Precipitated DNAs were quantified by ~~qRT-PCR~~ using MEX-3B promoter-specific primers covering TFII-I binding sites. (*B*) Human 293T cells transfected with pcDNA3.1(+)-TFII-I and siCBX4, together with firefly luciferase reporter and pRL-tk-Renilla plasmids for 24 hours. (*C*) IB analysis of TFII-I protein concentrations in HBE cells treated with HDM, siNC, or siCBX4. (*D*) Lung sections were stained with TFII-I antibody by immunohistochemistry. (*E*) Enhanced TFII-I SUMOylation in HDM-treated HBE cells. HDM-treated HBE cells were subjected to IP with anti–TFII-I followed by IB analysis with anti-SUMO1 and anti-SUMO2/3 antibody. (*F*) Decreased TFII-I SUMOylation in BEAS2B after CBX4 knockout (KO). Cell extract was subjected to IP with anti–TFII-I followed by IB analysis with anti-SUMO1 antibody after CBX4 KO. (*G*) Colocalization of SUMO1 and TFII-I in HDM-treated HBE cells was determined by immunofluorescence staining of SUMO1 and TFII-I. (*H*) Colocalization of SUMO1 and TFII-I in HBE cells transfected with siCBX4 was determined by immunofluorescence staining of SUMO1 and TFII-I. (*I*) ChIP assay with anti–TFII-I antibody in HBE cells transfected with the indicated plasmids for 48 hours. Precipitated DNAs were quantified by ~~qRT-PCR~~ for promoter regions of the MEX-3B gene. (*J*) Fold change of relative luciferase activity against lane 1 in human 293T cells transfected with pcDNA(+)-TFII-I and WT or CBX4 mutants, firefly luciferase reporter, and pRL-tk-Renilla plasmids for 24 hours. Data are presented as mean ± SEM. Images show representative results for one of three or more experimental replicates. (*A*) Unpaired two-tailed Student's *t* test was used. (~~*B–D, I,* and *J*~~) One-way ANOVA with Bonferroni's *post hoc* test was used. ~~$^{*}P < 0.05$ and $^{**}P < 0.01$~~.

we suspected that CBX4 might alter the level of TFII-I SUMOylation and therefore enhance its transcriptional activity. We observed that CBX4 knockdown caused a significant reduction of TFII-I binding to MEX-3B promoter and transcriptional activity (Figures 7A and 7B). Interestingly, HDM stimulation or CBX4 knockdown did not alter TFII-I expression in HBE cells (Figure 7C). Consistently, degrees of TFII-I expression were similar in control, HDM-treated, and 2-D08–treated murine airway epithelium (Figure 7D). These results suggest that CBX4 regulates only TFII-I transcriptional activity, not its expression. To confirm whether CBX4 regulates TFII-I transcriptional activity through SUMOylation, the degree of TFII-I SUMOylation was measured by co-IP in HDM-stimulated HBE cells. We observed an enhanced interaction between TFII-I and SUMO1 after HDM stimulation in HBE cells and a decreased interaction after CBX4 knockout in BEAS2B cells (Figures 7E and 7F). Furthermore, proximity ligation assays, a visualization method of detecting protein interactions, also confirmed these results (Figure E4). Similarly, colocalization of TFII-I and SUMO1 increased upon HDM stimulation and decreased upon CBX4 knockdown (Figures 7G and 7H). Next, we investigated whether CBX4 regulation of TFII-I transcription activity is dependent on the SIM structure of CBX4. For convenience of transfection, human 293T cells were transfected with plasmids expressing TFII-I and different mutant forms of CBX4. ChIP and luciferase reporter gene assays showed that overexpression of CBX4 promoted TFII-I binding to the MEX-3B promoter and transcription activity, and this effect persisted with the transfection of CDM-CBX4, but not △SIM1/2-CBX4 (Figures 7I and 7J). These observations support the hypothesis that CBX4 increases TFII-I SUMOylation and enhances the binding of TFII-I to the MEX-3B promoter, resulting in an increase in TFII-I–mediated MEX-3B transcription.

Discussion

For the first time, we have reported that SUMOylation was enhanced in HDM-induced allergic asthma epithelium and that inhibiting SUMOylation reduced airway inflammation, mucus production, and AHR. Furthermore, we identified CBX4 as a critical SUMOylation E3 ligase that regulated lfTSLP expression by promoting lfTSLP translation through the TFII-I–MEX-3B axis. These results indicate that inhibition of SUMOylation may alleviate lfTSLP-mediated allergic airway inflammation.

TSLP is reported to be involved in the regulation of inflammatory processes occurring at barrier surfaces. For example, a significant upregulation was observed in asthma, atopic dermatitis, and ulcerative colitis (33–35). Harada and colleagues provided evidence for the existence of two different isoforms of TSLP (lfTSLP and sfTSLP) in HBE cells (8). It has been reported that the expression of lfTSLP is upregulated, whereas expression of sfTSLP is unaffected, in airway epithelium challenged with polyinosinic-polycytidylic acid and HDM (8, 11). However, the exact mechanism behind this difference in expression remains unclear. Previous studies focused on the differences in their gene promoters (SNPs and transcription factors) (8, 36). However, little is known about their post-transcriptional regulation. In this study, we identified a novel post-transcriptional modification mechanism that specifically regulated lfTSLP, but not sfTSLP, expression. We observed that the SUMOylation E3 ligase, CBX4, could promote lfTSLP expression but had no effect on sfTSLP expression. In fact, CBX4 was not only a SUMOylation E3 ligase but also a member of PRCs that exerted its polycomb and nonpolycomb SUMOylation E3 ligase activities function through the CDM in the N-terminus and two SIMs (SIM1/2), respectively (19). Interestingly, we found that CBX4 regulated lfTSLP expression through its SUMOylation E3 ligase activity, but not polycomb function, in the present study and that CBX4 did not interact with lfTSLP directly. We subsequently identified that CBX4 regulates the RBP MEX-3B and that MEX-3B specifically binds to lfTSLP, but not sfTSLP, mRNA and promotes its translation.

MEX-3B is a member of MEX-3 family (MEX-3A, MEX-3C, and MEX-3D) of proteins that bind to specific mRNAs and regulates the expression of these proteins through their two KH-type RNA recognition domains (31). MEX-3B has been shown to regulate the post-transcriptional stability of IL-33 through its association with the 3′ UTR of IL-33 mRNA to inhibit its degradation in IL-33–mediated ovalbumin asthma model (30). Interestingly, we did not detect an upregulation of IL-33 in airway epithelium in our HDM-induced allergic asthma model and found that MEX-3B regulates lfTSLP RNA translation rather than affecting its stability. Moreover, database prediction suggested that MEX-3B might bind to the 5′ UTR of lfTSLP mRNA. These contradictory results may be explained by differences in asthma models. These results indicate that MEX-3B exerts multiple post-transcriptional functions in experimental asthma models.

Mechanistically, we identified CBX4 as a transcriptional coactivator of MEX-3B. Despite CBX4 knockdown resulting in the downregulation of MEX-3B mRNA and protein expression, we found that CBX4 did not bind to the MEX-3B promoter directly. Interestingly, we observed an interaction between CBX4 and TFII-I, a transcription factor of MEX-3B. CBX4 enhanced the degree of SUMOylation of TFII-I, which promoted its transcriptional activity. TFII-I has been reported to be involved in a wide range of human diseases, including neurocognitive disorders, systemic lupus erythematosus, and cancer (37). To our knowledge, this report is the first to demonstrate a role for TFII-I in TSLP-mediated allergic inflammation. However, several limitations of this study warrant discussion. For example, we failed to obtain samples from patients with asthma for this study. The expression of CBX4 in the airway epithelium of patients with asthma (including those with different inflammation phenotypes) merits additional study. In addition, further investigation of the airway epithelium from a CBX4 knockout murine asthma model is warranted.

Collectively, our findings have identified a CBX4–TFII-I–MEX-3B–lfTSLP axis involved in lfTSLP-mediated allergic airway inflammation, suggesting that substrates targeting the SUMO E3 ligase activity of CBX4 may be a novel target for the treatment of asthma. ■

Author disclosures are available with the text of this article at www.atsjournals.org.

Acknowledgment: The authors thank Prof. Tiebang Kang (Sun Yat-sen University) for pSIN-EF2-PURO-CBX4, pSIN-EF2-PURO-CBX4 (SIM1/2 mutant), and pSIN-EF2-PURO-CBX4 (CDM mutant) plasmids. The authors thank AiMi Academic Services (www.aimieditor.com) for English language editing and review services.

References

1. Adhikary PP, Tan Z, Page BDG, Hedtrich S. TSLP as druggable target – a silver-lining for atopic diseases? *Pharmacol Ther* 2021;217:107648.
2. Ito T, Wang YH, Duramad O, Hori T, Delespesse GJ, Watanabe N, *et al.* TSLP-activated dendritic cells induce an inflammatory T helper type 2 cell response through OX40 ligand. *J Exp Med* 2005;202:1213–1223.
3. Kim BS, Siracusa MC, Saenz SA, Noti M, Monticelli LA, Sonnenberg GF, *et al.* TSLP elicits IL-33-independent innate lymphoid cell responses to promote skin inflammation. *Sci Transl Med* 2013;5:170ra16.
4. Salter BMA, Smith SG, Mukherjee M, Plante S, Krisna S, Nusca G, *et al.* Human bronchial epithelial cell-derived factors from severe asthmatic subjects stimulate eosinophil differentiation. *Am J Respir Cell Mol Biol* 2018;58:99–106.
5. Astrakhan A, Omori M, Nguyen T, Becker-Herman S, Iseki M, Aye T, *et al.* Local increase in thymic stromal lymphopoietin induces systemic alterations in B cell development. *Nat Immunol* 2007;8:522–531.
6. Tanaka J, Watanabe N, Kido M, Saga K, Akamatsu T, Nishio A, *et al.* Human TSLP and TLR3 ligands promote differentiation of Th17 cells with a central memory phenotype under Th2-polarizing conditions. *Clin Exp Allergy* 2009;39:89–100.
7. Corren J, Parnes JR, Wang L, Mo M, Roseti SL, Griffiths JM, *et al.* Tezepelumab in adults with uncontrolled asthma. *N Engl J Med* 2017; 377:936–946.
8. Harada M, Hirota T, Jodo AI, Doi S, Kameda M, Fujita K, *et al.* Functional analysis of the thymic stromal lymphopoietin variants in human bronchial epithelial cells. *Am J Respir Cell Mol Biol* 2009;40:368–374.
9. Bjerkan L, Schreurs O, Engen SA, Jahnsen FL, Baekkevold ES, Blix IJ, *et al.* The short form of TSLP is constitutively translated in human keratinocytes and has characteristics of an antimicrobial peptide. *Mucosal Immunol* 2015;8:49–56.
10. Tsilingiri K, Fornasa G, Rescigno M. Thymic stromal lymphopoietin: to cut a long story short. *Cell Mol Gastroenterol Hepatol* 2017;3:174–182.
11. Dong H, Hu Y, Liu L, Zou M, Huang C, Luo L, *et al.* Distinct roles of short and long thymic stromal lymphopoietin isoforms in house dust mite-induced asthmatic airway epithelial barrier disruption. *Sci Rep* 2016;6: 39559.
12. Yang Y, He Y, Wang X, Liang Z, He G, Zhang P, *et al.* Protein SUMOylation modification and its associations with disease. *Open Biol* 2017;7:170167.
13. Varejão N, Lascorz J, Li Y, Reverter D. Molecular mechanisms in SUMO conjugation. *Biochem Soc Trans* 2020;48:123–135.
14. Fu J, Xiong Y, Xu Y, Cheng G, Tang H. MDA5 is SUMOylated by PIAS2β in the upregulation of type I interferon signaling. *Mol Immunol* 2011;48: 415–422.
15. Ran Y, Liu TT, Zhou Q, Li S, Mao AP, Li Y, *et al.* SENP2 negatively regulates cellular antiviral response by deSUMOylating IRF3 and conditioning it for ubiquitination and degradation. *J Mol Cell Biol* 2011; 3:283–292.
16. Kouzaki H, O'Grady SM, Lawrence CB, Kita H. Proteases induce production of thymic stromal lymphopoietin by airway epithelial cells through protease-activated receptor-2. *J Immunol* 2009;183: 1427–1434.
17. Kato A, Favoreto S Jr, Avila PC, Schleimer RP. TLR3- and Th2 cytokine-dependent production of thymic stromal lymphopoietin in human airway epithelial cells. *J Immunol* 2007;179:1080–1087.
18. Pichler A, Fatouros C, Lee H, Eisenhardt N. SUMO conjugation – a mechanistic view. *Biomol Concepts* 2017;8:13–36.
19. Ren X, Hu B, Song M, Ding Z, Dang Y, Liu Z, *et al.* Maintenance of nucleolar homeostasis by CBX4 alleviates senescence and osteoarthritis. *Cell Rep* 2019;26:3643–3656.e7.
20. Sanyal S, Mondal P, Sen S, Sengupta Bandyopadhyay S, Das C. SUMO E3 ligase CBX4 regulates hTERT-mediated transcription of CDH1 and promotes breast cancer cell migration and invasion. *Biochem J* 2020; 477:3803–3818.
21. Jiang N, Niu G, Pan YH, Pan W, Zhang MF, Zhang CZ, *et al.* CBX4 transcriptionally suppresses KLF6 via interaction with HDAC1 to exert oncogenic activities in clear cell renal cell carcinoma. *EBioMedicine* 2020;53:102692.
22. Gu L, Zhu N, Zhang H, Durden DL, Feng Y, Zhou M. Regulation of XIAP translation and induction by MDM2 following irradiation. *Cancer Cell* 2009;15:363–375.
23. Mitchell PD, O'Byrne PM. Epithelial-derived cytokines in asthma. *Chest* 2017;151:1338–1344.
24. Kumar A, Zhang KY. Advances in the development of SUMO specific protease (SENP) inhibitors. *Comput Struct Biotechnol J* 2015;13:204–211.
25. Rabellino A, Andreani C, Scaglioni PP. The role of PIAS SUMO E3-ligases in cancer. *Cancer Res* 2017;77:1542–1547.
26. Wotton D, Merrill JC. Pc2 and SUMOylation. *Biochem Soc Trans* 2007; 35:1401–1404.
27. Wang ZL, Li B, Luo YX, Lin Q, Liu SR, Zhang XQ, *et al.* Comprehensive genomic characterization of RNA-binding proteins across human cancers. *Cell Rep* 2018;22:286–298.
28. Licht K, Jantsch MF. Rapid and dynamic transcriptome regulation by RNA editing and RNA modifications. *J Cell Biol* 2016;213:15–22.
29. Oda T, Yamazumi Y, Hiroko T, Kamiya A, Kiriya S, Suyama S, *et al.* Mex-3B induces apoptosis by inhibiting miR-92a access to the Bim-3'UTR. *Oncogene* 2018;37:5233–5247.
30. Yamazumi Y, Sasaki O, Imamura M, Oda T, Ohno Y, Shiozaki-Sato Y, *et al.* The RNA binding protein Mex-3B is required for IL-33 induction in the development of allergic airway inflammation. *Cell Rep* 2016;16: 2456–2471.
31. Buchet-Poyau K, Courchet J, Le Hir H, Séraphin B, Scoazec JY, Duret L, *et al.* Identification and characterization of human Mex-3 proteins, a novel family of evolutionarily conserved RNA-binding proteins differentially localized to processing bodies. *Nucleic Acids Res* 2007; 35:1289–1300.
32. Tussie-Luna MI, Michel B, Hakre S, Roy AL. The SUMO ubiquitin-protein isopeptide ligase family member Miz1/PIASxβ /Siz2 is a transcriptional cofactor for TFII-I. *J Biol Chem* 2002;277:43185–43193.
33. Mitchell PD, O'Byrne PM. Biologics and the lung: TSLP and other epithelial cell-derived cytokines in asthma. *Pharmacol Ther* 2017;169: 104–112.
34. Park JH, Jeong DY, Peyrin-Biroulet L, Eisenhut M, Shin JI. Insight into the role of TSLP in inflammatory bowel diseases. *Autoimmun Rev* 2017;16:55–63.
35. Jariwala SP, Abrams E, Benson A, Fodeman J, Zheng T. The role of thymic stromal lymphopoietin in the immunopathogenesis of atopic dermatitis. *Clin Exp Allergy* 2011;41:1515–1520.
36. Fornasa G, Tsilingiri K, Caprioli F, Botti F, Mapelli M, Meller S, *et al.* Dichotomy of short and long thymic stromal lymphopoietin isoforms in inflammatory disorders of the bowel and skin. *J Allergy Clin Immunol* 2015;136:413–422.
37. Roy AL. Pathophysiology of TFII-I: old guard wearing new hats. *Trends Mol Med* 2017;23:501–511.

12

AUTHOR QUERIES

New Information for the ATS Journals
We are glad to inform you that most of the author-supplied artwork will now be redrawn in the new journal style.
Please check text, labels, and legends for accuracy and completeness. Check that colors noted in the figure legend match the colors in the figure and in the text of the article.

QA1 If you provided an ORCID ID at submission, please confirm that it appears correctly on the opening page of this article.

QA2 Please confirm that all necessary grants and funding sources are mentioned in the support footnote.

1 Au: Please define or expand "SUMO" at first use in the Abstract and in the Main Text, if applicable.

2 Au: Please verify definition of abbreviation muscle excess (MEX)-3B at first mention.

3 Au: Per journal style, citation of previous publication in preprint form was moved from the title page footnote to last sentence of Introduction section.

4 Au: IHC was introduced as the abbreviation for immunocytochemistry and also immunohistochemistry later, so for consistency, it is defined here at first mention as immunohistochemistry. Please confirm that this is meant each time the term is used.

5 Au: RT-PCR" stands for "reverse transcriptase–polymerase chain reaction" or "reverse transcription–polymerase chain reaction" (these are the same thing). Note that "real-time PCR" (also known as "quantitative PCR" and sometimes abbreviated as "qPCR") is different, and "qRT-PCR" (for quantitative reverse transcriptase–polymerase chain reaction) is a combination of the two. If "real-time" as the modifier of "PCR" (or of "qPCR"), then it should be spelled out. Please update if needed.

6 Au: Please verify expansion of SENPs as sentrin-specific proteases here and below in the same paragraph.

7 Au: Please verify definition of abbreviation protein inhibitor of activated STAT1 (PIAS1) at first mention.

8 Au: Please clarify what "its" refers to in the sentence beginning, "These data indicate that SIM-1/2 … "

9 Au: Please verify editing of sentence starting "Furthermore, HBE cells treated with … ."

10 Au: Please confirm expansion of "mRNP".

11 Au: Per journal style, in-text supplement citations have been designated with an "E" before the number; please amend the supplement accordingly and send corrected files (with a note detailing the changes that were made) to Ms. Mary Mobley (mmobley@thoracic.org).

12 Au: Original Reference 36 "Harada, Hirota, Jodo, Doi, Kameda, Fujita, et al., 2009" was a duplicate of reference 8, so it was deleted, citation was changed to 8, and subsequent citations and references were renumbered accordingly.

13 Au: Journal style is to define all abbreviations used in figure artwork and figure legends at the first occurrence. If an abbreviation is defined in Figure 1, we do not need to define it again in the remaining figure legends. Please verify that this style has been followed.

14 Au: In Fig. 1, please expand "SUMO" at first use.

15 Au: Please provide a revised figure with scale bar(s) as defined in the legend for Figure 1.

16 Au: Please confirm that all figures are original to this manuscript and have not previously appeared elsewhere in any print or electronic form (including the Internet). If they have appeared elsewhere, please provide the reference of the source, as well as confirmation that written permission to reprint (or reprint with modifications) has been received (or that the original is in the public domain). If the original is an ATS publication, permission is automatically granted.

17 Au: Please provide a revised figure with scale bar(s) as defined in the legend for Figure 2.

18 Au: Please provide a revised figure with scale bar(s) as defined in the legend for Figure 3.

19 Au: Please spell out siNC at first mention in Figures 4–7 legends.

20 Au: Fig. 7D, 7G, and 7H should have scale bars with their length defined in the legend. Please provide a revised figure with scale bars and add the lengths to the legend

21 Au: Please confirm addition of "*J*" after "and" in parentheses.

22 Au: Fig. 7F has *** and **** callouts that need to be defined in the legend.